SafeLand

Living with landslide risk in Europe: Assessment, effects of global change, and risk management strategies

7th Framework Programme
Cooperation Theme 6 Environment (including climate change)
Sub-Activity 6.1.3 Natural Hazards

Deliverable D2.11

QRA case studies at selected "hotspots"

WP 2.3 - Development of procedures for QRA at regional scale and European scale

REPORT OF THE ACTIVITIES

CARRIED OUT BY THE RESEARCH GROUP OF UNISA

Contributors: Leonardo Cascini, Settimio Ferlisi, Giuseppe Sorbino, Sabatino Cuomo

Introduction

This report summarises the results of the activities carried out by the research group of the University of Salerno (UNISA) with reference to the test site of Monte Albino (Nocera Inferiore, southern Italy). In particular, these activities dealt with the acquisition of the relevant input data and their use within advanced procedures aimed to the quantitative estimation of the risk to life loss posed by the different types of phenomena that could originate from Monte Albino hillslopes (i.e., hyperconcentrated flows, flowslides, landslides on open slopes).

1. Monte Albino case study

The selected test site of Monte Albino (40°43'N, 14°38'E), located in the municipality of Nocera Inferiore (southern Italy), extends over a total area of about 400 ha, from 890 m a.s.l. to 90 m a.s.l. (Fig. 1). Along the hillslope 10 catchments can be individuated as well as 10 open slopes (triangular facets), located in the lower portions of the relief (below 330 m a.s.l.). In March 2005, one of these open slopes was affected by a first-failure landslide (Fig. 2) which caused 3 fatalities and the destruction of some buildings.

Figure 1. Study area.

In order to define the geological setting as well as to deepen the knowledge of the different types of phenomena which can occur on the slopes, in-situ tests, field surveys and studies were firstly carried out following a multidisciplinary approach (involving competences on historical data

treatment, geology, morphology, hydrogeology, geotechnics, geomatics, geostatistics, etc.). The main results achieved during this preliminary step of the work are herein presented.

Figure 2. Frontal view of the debris avalanche occurred on March 2005.

2. Analysis of historical incident data

2.1. Documentary sources

For the events preceding the 18th century the documentary sources consisted on historical-literary books (Orlando, 1884; Cimmelli, 1990; Pucci, 1995) and technical reports (Beguinot, 1957; Marciani, 1930; D'Elia, 1994).

For the 19th century, historical incident data were recovered in the documents of the "Intendenza del Regno delle Due Sicilie (Sezione Opere Pubbliche)", founded by the Bourbons in 1806, and housed in the State Archive of Salerno. These documents include the correspondence between the "Intendente" and the Mayors of the towns affected by landslides as well as appraisals for the reconstruction works following the catastrophic events.

In relation to the 20th century the main source is the report of the Operative Unit 2.38 (1998) of the University of Salerno, synthesised by Migale e Milone (1998), in which the results of a historical research on first-failure landslides occurred in Campania region in a time period spanning from the end of the 16th century up to now are summarised.

2.2. Results of the analyses

From a deep analysis of the contents of the recovered historical documents it is argued that the events occurred on 18th and 19th centuries can be associated to the occurrence of hyperconcentrated

flows (Costa, 1988). On the other hand, the incident data referring to the 20th century (also considering the landslides occurred on March 2005) can be linked to first-failure landslides on open slopes while historical information about flowslide phenomena (Hutchinson, 1988) are lacking.

2.2.1. Hyperconcentrated flows

With reference to the hyperconcentrated flows, information furnished by the documentary sources essentially deals with the consequences related to the occurrence of the phenomena at hand. In particular, as far as the incident data of the 18th century are concerned, the described consequences refer to some built-up areas of Nocera de' Pagani (this is the name of the Municipality at that time) and to the site called "Vescovado" (Fig. 3); furthermore, these consequences seem to have been more severe, in terms of recorded damage, than those caused by the events occurred in the 19th century. In this regard, it can be observed that in the 18th century the described consequence are often due to adverse events originated from the Monte Albino hillslopes (i.e., the hyperconcentrated flows) as well as to flooding phenomena.

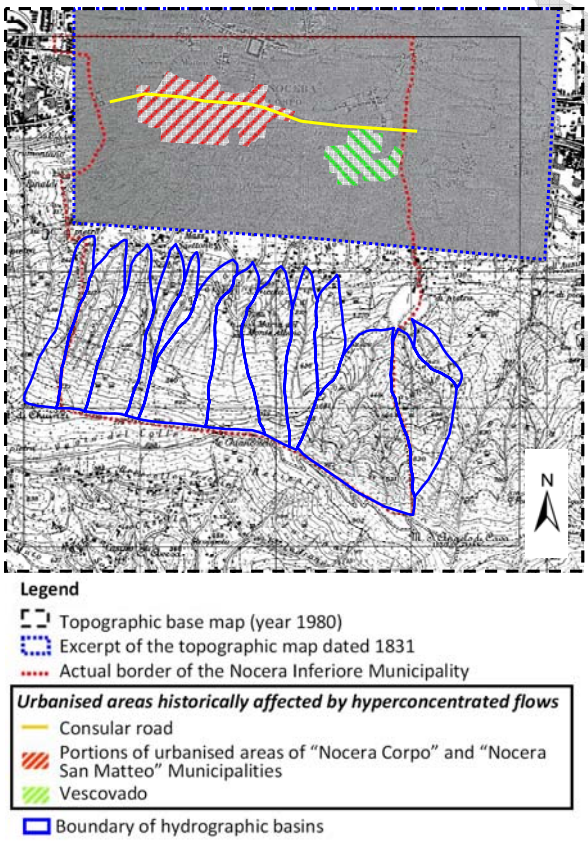

Figure 3. Urbanised areas affected by hyperconcentrated flows occurred during the 18th and the 19th centuries.

At the beginning of the 19th century, as required by the King of Bourbons Ferdinand IV who experienced the block of the consular road owing the event of 1804, some hydraulic control works

were built in the flat areas (Orlando, 1884; Marciani, 1930; Beguinot, 1957). In the following, thanks also to the existence of these mitigation measures, the consequences related to the occurrence of the hyperconcentrated flows were limited to troubles in accessing some sections of the consular road, near the built-up areas.

Finally, it is worth noting that some documents also furnish information about the cost (in ducats) required for the removal of transported sediments on the road.

The cumulative curve of past hyperconcentrated flow events (Fig. 4) is characterised by a stepped shape during the time period (from 1707 to 1846) for which historical incident data are available.

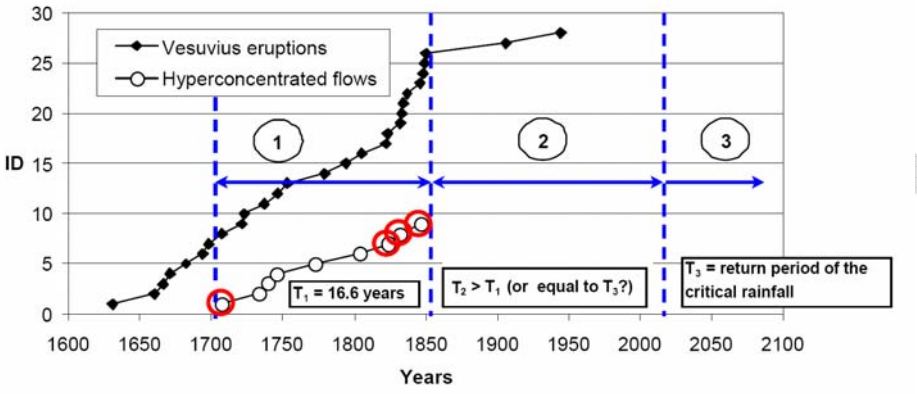

Figure 4. Cumulative distributions of: *i)* Vesuvius explosive eruptions occurred from 1631 up to now; ii) hyperconcentrated flow incident data (events occurred after the Vesuvius eruptions are circled in red).

Figure 4 also shows that the occurrence of the events may be correlated with the explosive eruptions of the Vesuvius volcano; in particular, between the 1811 and 1848, during a period of intensive strombolian activity of the volcano (Scandone et al., 2008), n. 3 hyperconcentrated flow events were recorded (Table I).

With reference to the seasonal distribution of the past events, Figure 5 shows that the recorded incident data concentrate between October and January, with a maximum in November. In this regard, the occurred phenomena can be ascribed to: *i)* the availability of pyroclastic soils over the hillslopes (Fig. 6a), transported by the winds blowing toward the eastern sectors (northeast–southeast) during the Autumn-Winter periods are (Rolandi et al., 2007); *ii)* the washing operated by rainfall of short duration and high intensity.

Table I. Recorded incident data of hyperconcentrated flows occurred from 1707 to 1846, with indication of the affected areas.

ID	Day	Month	Year	Affected area
1	-	11	1707	All the town(*)
2	11	11	1733	All the town and the consular road
3	24	10	1739	All the town and the "Vescovado"
4	02	12	1745	All the town and the "Vescovado"
5	11	11	1773	All the town and the "Vescovado"
6		1	1804	The consular road
7	24	1	1823	The consular road
8	30	11	1832	The consular road
9	02	10	1846	The consular road

(*) The term "town" indicated the built-up area at the time when the phenomena occurred.

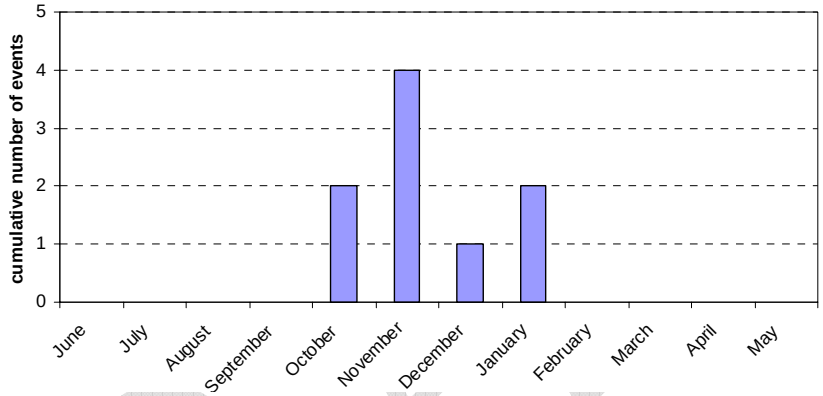

Figure 5. Monthly distribution of the hyperconcentrated flows which, in the past, interested the Monte Albino hillslopes.

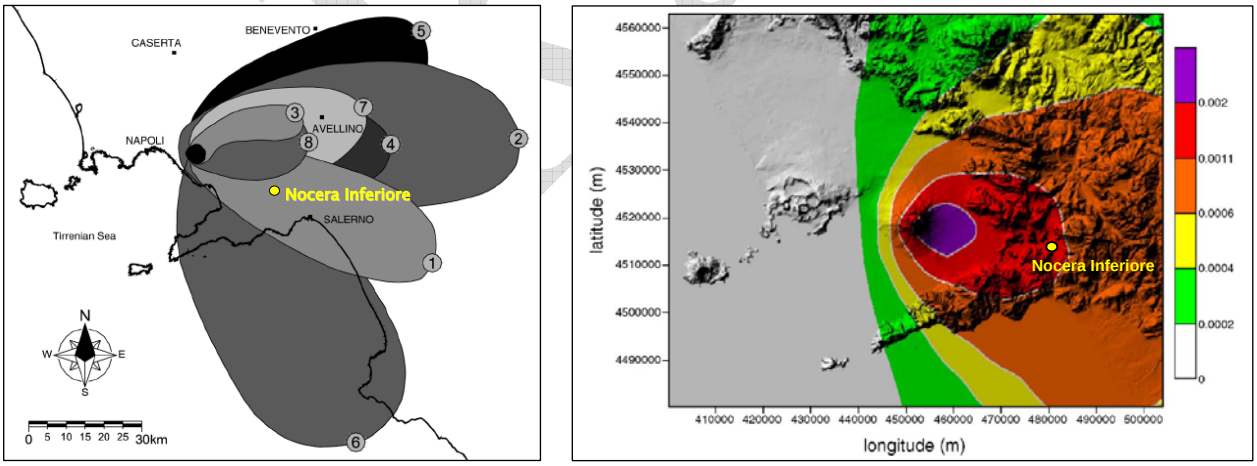

Figure 6. a) Distribution map of pyroclastic fall deposits of the Somma-Vesuvius deposited in the last 25 ka BP. Each lobe consists of air fall tephra 10 cm thick from a single Plinian eruption. Numbers are arranged according to the chronological sequence of the eruption. (1) 25.000 anni B.P.; (2) 18.000 anni B.P.; (3) 16020 anni B.P; (4) 8000 anni B.P.; (5) 3550 anni B.P.; (6) A.D. 79; (7) A.D. 472; (8) A.D. 1631 *(modified from Rolandi et al., 2007)*. b) Fall-out hazard map for Vesuvius eruptions. The maps are computed, by several tens thousands of computer simulations, on the basis of the observed wind velocity and direction between 0 and 35 km of height and their relative occurrence, considering all the eruption types with their statistics distributions, according to the volcanological records. The values are the yearly probabilities of a tephra load exceeding 200 kg/m^2 (producing the collapse of most roofs) *(modified from De Natale et al., 2006)*.

The previous considerations allow the assumption of some hypotheses on the return period of the hyperconcentrated flow events (Fig. 4). In particular, with reference to the time period ΔT_1 spanning from 1707 to 1846 (ΔT_1 = 140 years), it can be assumed that the average return period T_1 – in the hypothesis that the database is complete – is equal to 16.6 years (140 years/9 events). If the ΔT_2 time period (from 1846 up to now) is considered, owing to the reduced recurrence of strombolian eruptions, the average return period T_2 of the hyperconcentrated flows is greater than T_1. Moreover, since their occurrence is related to erosive phenomena rather than washing, it can be assumed that T_2 can be equal to the return period T_3 of the triggering rainfall events.

Tanking into account the low annual probability that, according to De Natale et al. (2006) can be associated with the occurrence of air-fall pyroclastic deposits (Fig. 6b), future hyperconcentrated flows will be characterised by a average return period equal to T_3, being their occurrence mainly related to erosive phenomena.

2.2.2. First-failure landslides on open slopes

With reference to the first-failure landslides on open slopes occurred from 1935 up to now, on the basis of the available data (Table II), it can be observed that the average time period of recurrence equals 18.5 years. This value could be unsafe, being the estimation of T carried out without considering the role played by the anthropogenic factors in predisposing this kind of instability phenomena.

Table II. Recorded incident data of landslides on open slopes occurred from 1935 to 2005, with indication of the consequences to the exposed persons and properties.

ID	Day	Month	Year	Fatalities/Endangered sites
1	-	-	1935	-
2	24	10	1954	-
3	-	-	1958	-
4	4	3	2005	3 fatalities/some houses destroyed

3. In-situ tests

The Monte Albino massif is constituted by a carbonatic bedrock covered by reworked and in-situ pyroclastic deposits originated from the air-fall deposition of the materials produced by the explosive activity of the Somma-Vesuvius volcanic complex. In order to acquire all over the Monte Albino hillslopes the geotechnical dataset (soil cover thickness, soil stratigraphy, physical and

mechanical characteristics of the pyroclastic soils, etc.) to be used within the advanced methods useful for QRA purposes (Corominas and Mavrouli, 2011), the following in-situ tests were carried out from November to December 2010:

- n. 68 Seismic field tests;
- n. 40 Dynamic penetration tests (DL030);
- n. 20 Undisturbed soil sampling;
- n. 70 Man-made pits (with detailed soil stratigraphy);
- n. 1,030 Iron-rod drillings;
- n. 54 Suction measurements via quick-draw tensiometers.

Figure 7 shows the map of the test sites at the Monte Albino hillslopes.

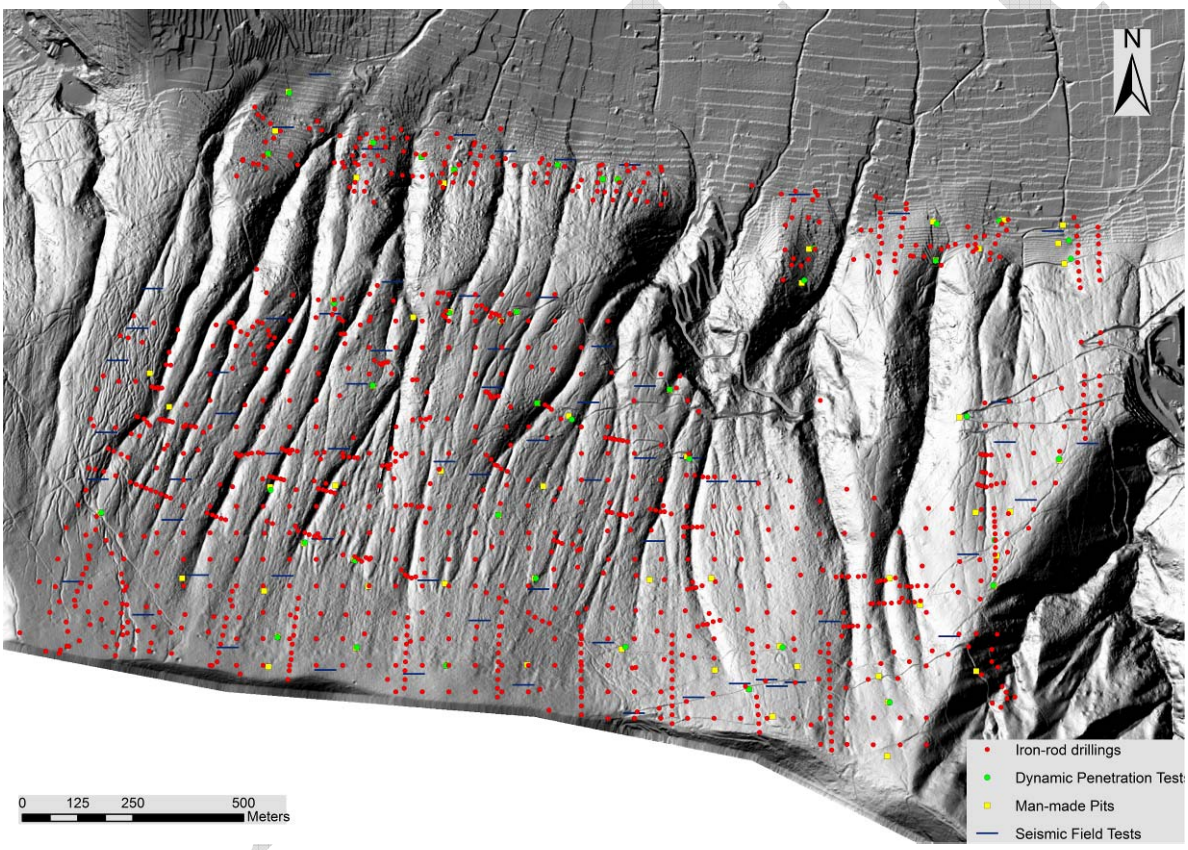

Figure 7. DTM obtained on the basis of the data achieved via a LIDAR survey technique (Avioriprese s.r.l., edition of 2005, 1:1,000 scale), with indication of the sites where the in-situ tests were carried out (*from the presentation given by Prof. Leonardo Cascini during the 1st meeting of the participatory process in Nocera Inferiore – April 14, 2011*).

4. Geological setting

On the basis of the in-situ test results and the field observations on selected areas as well as of the morphological analysis extensively carried out on both topographic maps at different scales and

high-detail orthophotos, the thickness distribution of the pyroclastic deposits has been estimated and mapped in the study area. The spatial distribution of the thickness classes is controlled by the morphology of the slope. In particular, the thickness of the pyroclastic deposits reach values of 4 m in the median part of the western sector of the slope where the slope angles range between 20 and 30 degrees; on the contrary, the thickness values do not exceed 1.5 m in the eastern part of the slope where slope angles attain the highest values. Moreover, it must be observed that the main vertical discontinuities of the pyroclastic deposits correspond to: *i)* "scarps in calcareous rocks" (usually having a structural control due to the presence of fault scarps or thick strata heads) and *ii)* "erosion scarps along the gullies" (mainly originated by the erosive processes that grooved the pyroclastic covers and, in some cases, allowed the uncovering of the carbonatic bedrock often in correspondence of the buried tectonic elements).

Moving from the upper part to the toe of the slope, it is possible to recognise – in the western part of the Monte Albino hillslope – the presence of morphological concavities filled by pyroclastic soils and prone to first-failure phenomena. On the contrary, in the eastern part, streams cutting directly into the carbonatic bedrock are found. In the lateral sectors of the gullies, in the inter-rill areas and along the open slopes there is the presence of morphological elements probably related to landslide and erosive processes. The area at the toe of the slope shows a complex array of fans of different origin, on the top of which lies a part of the urbanized area of the Nocera Inferiore municipality.

Finally, it is worth to observe that the study area corresponds to the northern part of the hydrogeological Unit of the Lattari Mounts, where the groundwater regimen is conditioned by the main tectonic structures originating springs in the lower part of the slope; also ephemeral springs can be found in the upper part of the slope related to suspended groundwaters.

5. Prevailing flow-like mass movements

Owing to the above described geological predisposing factors and taking into account the results of the historical analysis, it can be argued that the Monte Albino hillslopes are prone to different types of rainfall-induced flow-like mass movements (Hutchinson, 2004), namely: hyperconcentrated flows, landslides on open slopes and flowslides.

The *hyperconcentrated flows*, as already outlined, essentially relate to erosion processes originated by heavy rains and affect the pyroclastic soils cover along rills as well as on the inter-rills areas.

The *landslides on open slopes* affect the triangular facets located at the base of the slope; they have similar characteristics to the phenomenon occurred on March 2005 and are classifiable as "debris avalanches" (Hungr et al., 2001).

Finally, in spite of the lack of historical incident data, *flowslides* can be triggered in some areas – e.g., in the so-called "Zero Order Basins" (Dietrich et al., 1986; Cascini et al., 2008) – located in the upper part of Monte Albino massif. The magnitude of the displaced masses could be significantly increased by the materials eventually entrained during the post-failure and propagation stages.

6. Quantitative assessment of the risk to life loss

Quantitative Risk Assessment (QRA) has become an indispensable tool for management of landslide hazard and for planning risk mitigation measures at detailed scale (Fell et al. 2008). The framework for the use of QRA for landslides and engineered slopes has been recently reviewed by Fell et al. (2005). In particular, this framework comprises three main components, i.e.: *Risk analysis; Risk assessment; Risk management*.

Risk analysis includes hazard and consequence analyses. *Hazard analysis* is the process of identification and characterisation of existing and/or potential landslides together with evaluation of their corresponding frequency of occurrence. *Consequence analysis*, in turn, involves:

(a) Identifying and quantifying the elements at risk including property and persons.
(b) Assessing temporal spatial probabilities for the elements at risk;
(c) Assessing vulnerability of the elements at risk.

Risk estimation is the final step of the *Risk analysis* and essentially consists in the risk calculation through a probabilistic equation. For instance, the annual probability that *a particular person* (e.g. the most exposed one to the landslide risk) may lose his/her life $P^i_{(LOL)}$, in general, can be calculated through the formula (Fell et al., 2005):

$$P^i_{(LOL)} = P^i_{(R)} \times P^i_{(T:R)} \times P_{(S:T)} \times V^i_{(D:T)} \quad (1)$$

where $P^i_{(R)}$ is the frequency of the landslide events of a given *i*-magnitude; $P^i_{(T:R)}$ is the probability of the landslide reaching the element at risk; $P_{(S:T)}$ is the temporal spatial probability of the element at risk; $V^i_{(D:T)}$ is the vulnerability of the person with respect to the landslide event.

If the element at risk is exposed to a number of different sizes of landslides of the same classification system, the risks pertaining to each landslide size can be summed in order to obtain the total risk (Corominas et al., 2005). In such a case, the expression (1) can be more conveniently rewritten as:

$$P_{(LOL)} = \sum_{i=1}^{n} \left(P^i_{(R)} \times P^i_{(T:R)} \times P_{(S:T)} \times V^i_{(D:T)} \right) \quad (2)$$

being *n* the number of landslide volume classes.

According to Fell et al. (2005), *Risk assessment* involves taking the outputs from the *Risk analysis* and comparing them (*risk evaluation*) against values judgements and risk tolerance criteria to determine if the risks are low enough to be tolerable. The main goal is to determine the best decision option for development and/or risk mitigation considering all objectives.
Once the risk posed by the landslide in a given area is assessed, *Risk management* identifies the measures that may be taken to mitigate landslide risk to the community, if necessary. In this regard, different strategies can be considered and, according to Dai et al. (2002) they may be grouped into: *i)* planning control, *ii)* engineering solution, *iii)* acceptance, *iv)* monitoring and warning systems.

In the following, with reference to the different kinds of flow-like mass movements that can affect the Monte Albino hillslopes (including flooding phenomena), the adopted procedures and the main results achieved in the quantitative risk – to life loss – assessment and related zoning are briefly summarised.

6.1 Risk to life loss posed by the hyperconcentrated flows

As far as the hyperconcentrated flows are concerned, the main purpose of the QRA analyses consisted on the assessment of the risk to life loss posed by the above phenomena to persons living in the urbanised area at the toe of the Monte Albino massif (Nocera Inferiore, Salerno Province). In order to pursue this goal, the methodological approach provided by Fell et al. (2005) and further deepened by Corominas and Mavrouli (2011) was followed.

6.1.1. Hazard analysis: danger characterization

For QRA purposes hyperconcentrated flows patterns have been evaluated for each basin via the FLO-2D numerical code (O'Brien et al., 1993), referring to a rainfall event having T = 200 years (namely, the return period to be considered – in Italy – for the design of hydraulic control works) by using a DTM – of squared cells of 5 m x 5 m – obtained via the data achieved by a LIDAR survey .
A synthesis of the input data, in terms of water (V_{water}) and sediment (V_{sed}) volumes, for each of the involved basins, is reported in Table III. It is worth noting that the water volumes were computed on the basis of the VAPI procedure given, for the Campania region, by Rossi and Villani (1995). As far as sediment volumes are concerned, they were estimated thanks to the erosion theory provided by Hungr (1995).

Table III. Input data considered in the analyses dealing with the propagation stage of the hyperconcentrated flows.

Basin	V_{sed} (m^3)	V_{water} (m^3)	V_{tot} (m^3)	V_{sed}/V_{tot}
1	2069.5	3953	6023	0.34
2	2982.5	7052	10035	0.30
3	3119.5	6890	10010	0.31
4	1689.0	3038	4727	0.36
5	705.5	1778	2484	0.28
6	4068.0	7405	11473	0.35
7	2016.0	4918	6934	0.29
8	2964.0	8237	11201	0.26
9	799.0	4586	5385	0.15
10	679.0	2775	3454	0.20

In order to take into account the uncertainties related to rheological properties of the involved mixtures, the following combinations of the parameters τ (shear strength at the base of the propagating flow) and η (dynamic viscosity) were considered:

Scenario 1:

- τ = 1 kPa
- η = 1 Pascal·sec

Scenario 2:

- τ = 1 kPa
- η = 0.1 Pascal·sec

Scenario 3:

- τ = 0.1 kPa
- η = 0.1 Pascal·sec

Finally, areas occupied by the buildings were assumed as "blocked" cells.

Results of FLO-2D numerical code are furnished in terms of depth and velocity of hyperconcentrated flows fronts impacting the exposed houses. In particular, maximum values of both depths and velocities dealing with the cells located around each facility were considered for the analysis purposes. In particular, based on the numerical results, it was estimated that the probability $P_{(T:L)}$ of hyperconcentrated flow phenomena reaching the elements at risks (the houses and their occupants) is equal to:

- 1 if the propagating flows impacts a given house in all the considered scenarios;
- 0.66 if the propagating flows impacts a given house in two scenarios over three;
- 0.33 if the propagating flows impacts a given house in only one scenario.

6.1.2. Hazard analysis: frequency analysis

Complete landslide records covering a long time span may be used to perform the probabilistic analyses. According to Corominas and Moya (2008), two probability distributions can be used to assess the annual probability of occurrence of landslides: the binomial distribution and the Poisson distribution. The binomial distribution can be applied for the cases considering discrete time intervals and only one observation for interval (usually a year), as is typically made in flood frequency analysis. The annual probability of a landslide event of a given magnitude which occurs on average one time each T years is:

$$P_{(N = 1;\, t = 1)} = 1/T = P_{(L)}$$

where T is the return period of the event and $P_{(L)}$ the expected frequency for future occurrences.

Then, for the problem at hand in which 10 basins may be *potentially* involved by hyperconcentrated flow as a consequence of a rainfall event of return period T = 200 years, the following frequency value results:

$$P_{(L),200} = 1/200 \cdot 0.5 = 0.0025 \text{ events/year};$$

being 0.5 the (assumed) probability that a given basin should be *really* involved by a hyperconcentrated flow during the above rainfall event.

6.1.3. Consequence analysis

The $P_{(S:T)}$ terms were computed on the basis of the age of the inhabitants. In particular, the adopted values are reported in the following Table IV. It is worth observing that, when information about people living in the impacted houses were lacking, it was safely assumed a $P_{(S:T)}$ value equal to 1.

Table IV. Temporal-spatial probability value adopted on the basis of the age of the inhabitants.

Age (years)	**$P_{(S:T)}$**
0 ÷ 5	1
6 ÷ 18	0.75
19 ÷ 65	0.5
66 ÷ 75	0.75
> 75	1

The social vulnerability factors $V_{(D:T)}$ for *persons most at risk living* within the potentially impacted buildings (i.e., having $P_{(T:L)} \neq 0$) have been assessed via a "direct approach" (Wong et al., 1997); the corresponding values are reported in the Table V as a function of the output data of the FLO-2D numerical code. In particular, these values correspond to the average maximum values of both depth

and velocity of hyperconcentrated flows fronts obtained with reference to the cells surrounding a given house.

Table V. $V_{(D:T)}$ values adopted with reference to the vulnerability of the person most exposed at the hyperconcentrated flow risk.

Case	flow depth h (m) / velocity v (m/s)	Adopted $V_{(D:T)}$ value
1. If the building is inundated with sediment-fluid mixture and the person have a high chance to be buried	$h \geq 1$ and $v \geq 5$	0.15
	$h \geq 1$ and $1 \leq v < 5$	0.1
	$0.5 \leq h < 1$ and $v \geq 5$	0.1
2. If the building is inundated with the sediment-fluid mixture and the persons have a low chance to be buried	$h \geq 1$ and $v < 1$	0.08
	$0.5 \leq h < 1$ and $1 \leq v < 5$	0.08
	$h < 0.5$ and $v \geq 5$	0.08
	$0.5 \leq h < 1$ and $v < 1$	0.05
	$h < 0.5$ and $1 \leq v < 5$	0.05
3. If the sediment-fluid mixture strikes the building only	$h < 0.5$ and $v < 1$	0.02

6.1.4. Risk estimation

The obtained results, in terms of individual risk to life, were summarised in a map (Fig. 8) showing, for each of the houses impacted by the hyperconcentrated flows, the corresponding $P_{(LOL)}$ referred to the person most at risk. It is worth noting that some of the most exposed persons have a risk higher than 10^{-4}/annum, namely the risk tolerability threshold established by the Geotechnical Engineering Office (1998) of Hong Kong.

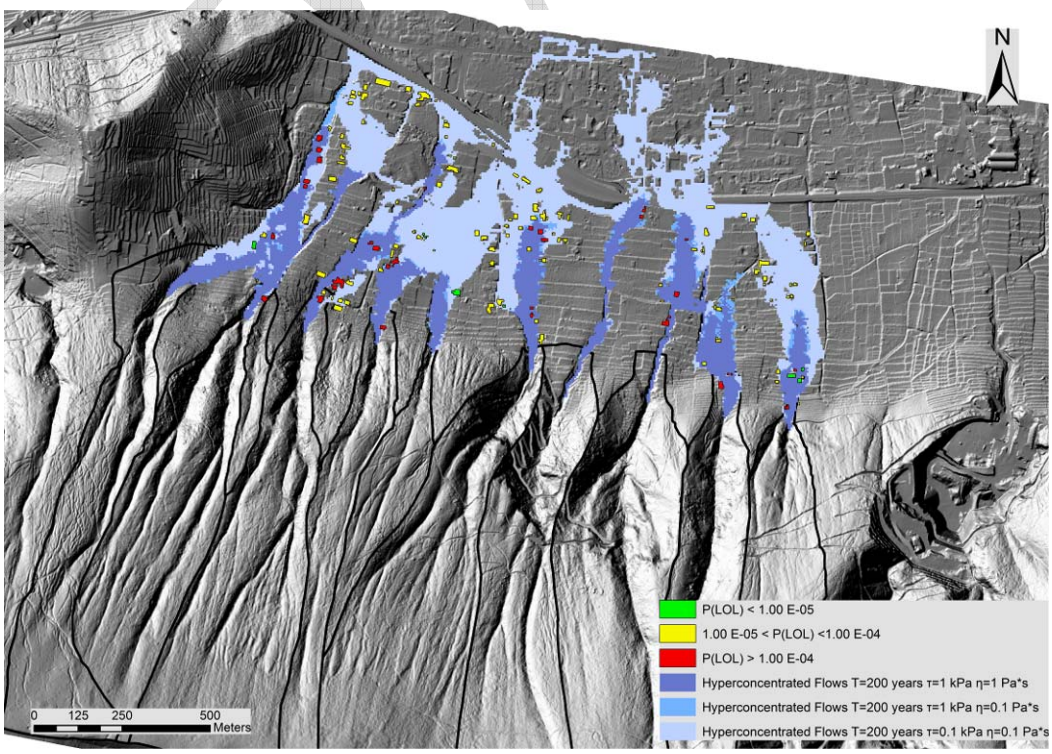

Figure 8. Map of the risk to life loss posed by the hyperconcentrated flows *(modified from the presentation given by Prof. Leonardo Cascini during the 3rd meeting of the participatory process in Nocera Inferiore – June 9, 2011).*

6.2 Risk to life loss posed by the flowslides

As far as the risk to life loss posed by the flowslides, the analyses were carried out similarly to those previously described for the hyperconcentrated flows.

Anyway, for rainfall events having a return period T = 200 years, the mobilised soil volumes at the source areas were obtained by using the TRIGRS physically-based model (Baum et al., 2002) as well as the Infinite Slope Model implemented in a GIS environment (Fig. 9).

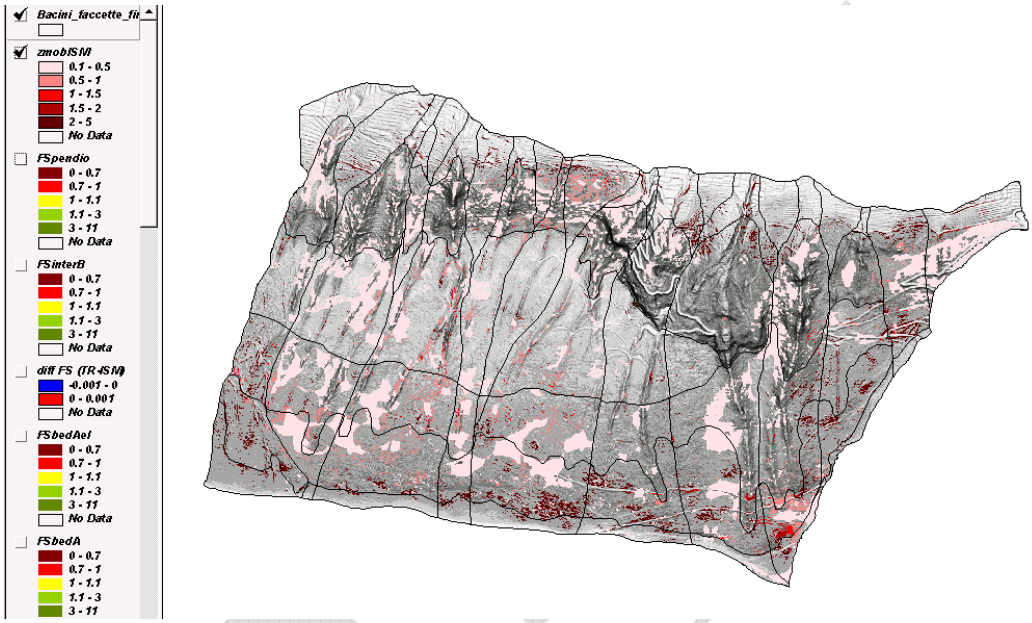

Figure 9. Stable (FS > 1) and unstable (FS ≤ 1) areas obtained via the use of the Infinite Slope Model for a rainfall event having a return period T = 200 years.

On the other hand, only one scenario of propagation stage (via the FLO-2D numerical code, assuming τ = 1 kPa and η = 2 Pascal·sec) was considered while the vulnerability values were assumed according to the information provided by the Table VI.

Table VI. $V_{(D:T)}$ values adopted with reference to the vulnerability of the person most exposed at the flowslide risk.

Case	flow depth h (m) / velocity v (m/s)	Adopted $V_{(D:T)}$ value
1. If the building is inundated with debris and the person have a high chance to be buried	h ≥ 1 and v ≥ 7	1
	h ≥ 1 and 3 ≤ v < 7	0.8
	0.5 ≤ h < 1 and v ≥ 7	0.8
2. If the building is inundated with debris and the persons have a low chance to be buried	h ≥ 1 and v < 3	0.4
	0.5 ≤ h < 1 and 3 ≤ v < 7	0.4
	h < 0.5 and v ≥ 7	0.4
	0.5 ≤ h < 1 and v < 3	0.2
	h < 0.5 and 3 ≤ v < 7	0.4
5. If the debris strikes the building only	h < 0.5 and v < 3	0.05

The obtained results, in terms of individual risk to life, were summarised in a map (Fig. 10) showing, for each of the houses impacted by the flowslides, the corresponding $P_{(LOL)}$ referred to the person most at risk. Obviously, passing from the hyperconcentrated flow to flowslide phenomena, the number of the most exposed persons having a risk higher than 10^{-4}/annum strongly increases as $V_{(D:T)}$ values increase.

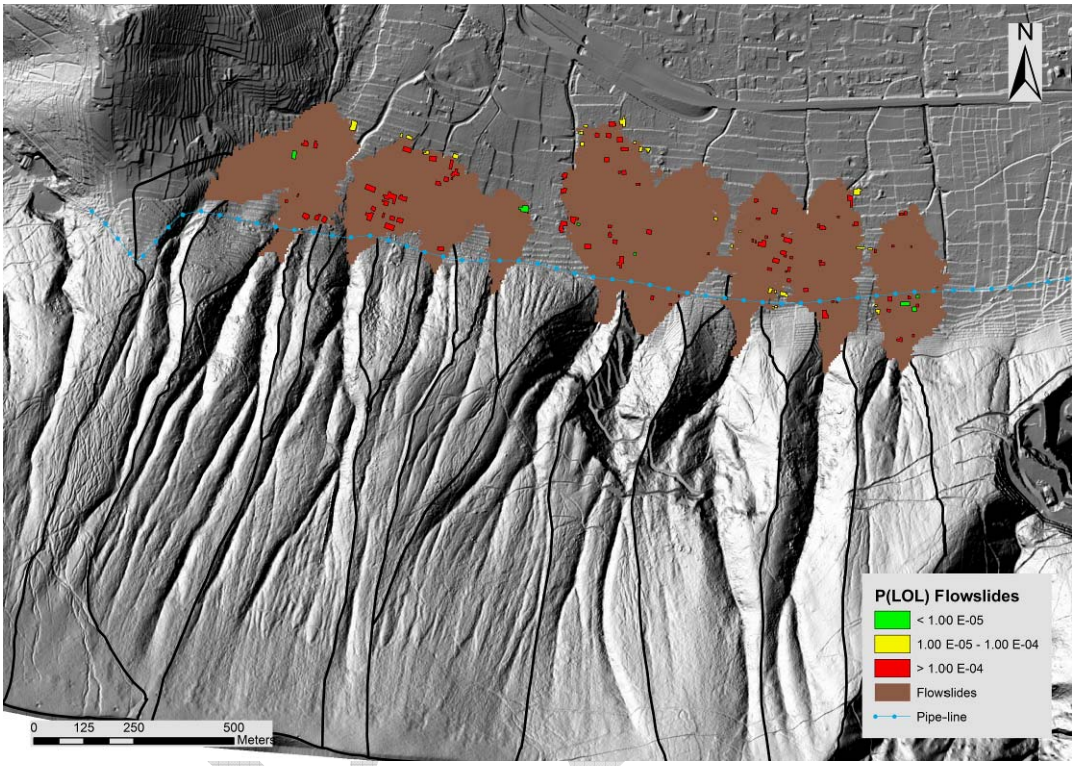

Figure 10. Map of the risk to life loss posed by the flowslides *(modified from the presentation given by Prof. Leonardo Cascini during the 3rd meeting of the participatory process in Nocera Inferiore – June 9, 2011).*

6.3 Risk to life loss posed by the landslides on open slopes

Referring the risk to life loss posed by the landslides on open slopes, the run-out distance was computed by adopting a heuristic criterion, taking into account the shape of the ancient alluvial fans.

The landslide frequency $P_{(L)}$ was computed considering that, on the basis of historical information, 4 events occurred, over a period of 80 years, in a total of 10 open slopes. As a consequence:

$$P_{(L)} = (4/80)\cdot(1/10) = 0.005/\text{annum}$$

The vulnerability $V_{(D:T)}$ was, in turn, estimated considering the criterion explained in Figure 11, similar to that proposed by Wong (2005).

The obtained results, in terms of individual risk to life, were summarised in a map (Fig. 12) showing, for each of the houses impacted by the flowslides, the corresponding $P_{(LOL)}$ referred to the person most at risk. It is worth to observe that the most exposed persons have, in the case of

landslides on open slopes, the highest risk among those obtained for the different kind of flow-like mass movements that could originate from Monte Albino hillslopes.

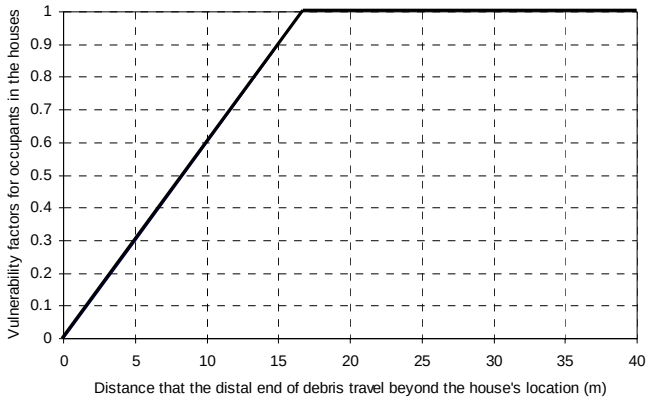

Figure 11. Vulnerability factors.

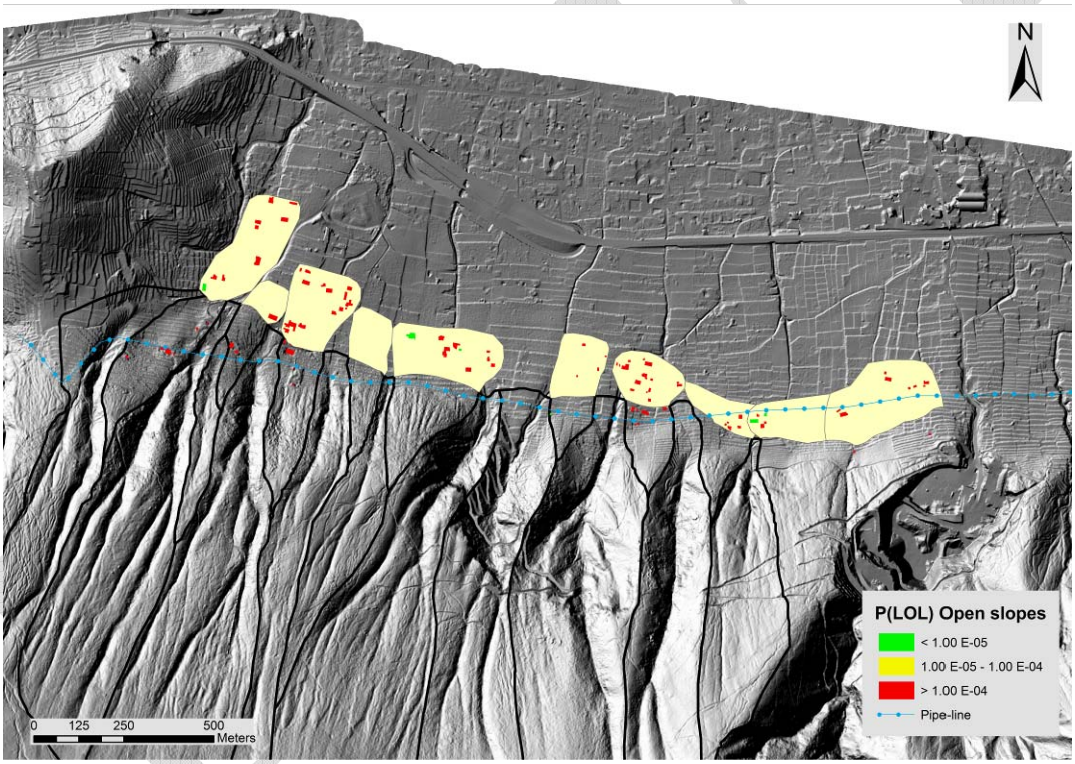

Figure 12. Map of the risk to life loss posed by the landslides on open slopes *(modified from the presentation given by Prof. Leonardo Cascini during the 3rd meeting of the participatory process in Nocera Inferiore – June 9, 2011).*

6.4 Risk posed by the flooding phenomena

As far as the risk to life loss posed by the flooding phenomena is concerned, a rainfall event having a return period T = 100 years was considered for the analysis purposes. On the basis of the results obtained via the FLO-2D numerical code, the vulnerability values were assumed according to the information provided by Table VII.

The obtained results, in terms of individual risk to life, were summarised in a map (Fig. 13) showing, for each of the houses impacted by the flooding phenomena, the corresponding $P_{(LOL)}$ referred to the person most at risk. It is worth noting that the obtained risk values are tolerable for all persons most at risk.

Table VII. $V_{(D:T)}$ values adopted with reference to the vulnerability of the person most exposed at the flooding risk.

Case	flow depth h (m) / velocity v (m/s)	Adopted $V_{(D:T)}$ value
1. If the building is inundated with the water and the person have a high chance to be buried	$h \geq 1$ and $v \geq 5$	0.1
	$h \geq 1$ and $1 \leq v < 5$	0.05
	$0.5 \leq h < 1$ and $v \geq 5$	0.05
2. If the building is inundated with the water and the persons have a low chance to be buried	$h \geq 1$ and $v < 1$	0.025
	$0.5 \leq h < 1$ and $1 \leq v < 5$	0.025
	$h < 0.5$ and $v \geq 5$	0.025
	$0.5 \leq h < 1$ and $v < 1$	0.01
	$h < 0.5$ and $1 \leq v < 5$	0.01
3. If the water strikes the building only	$h < 0.5$ and $v < 1$	0.005

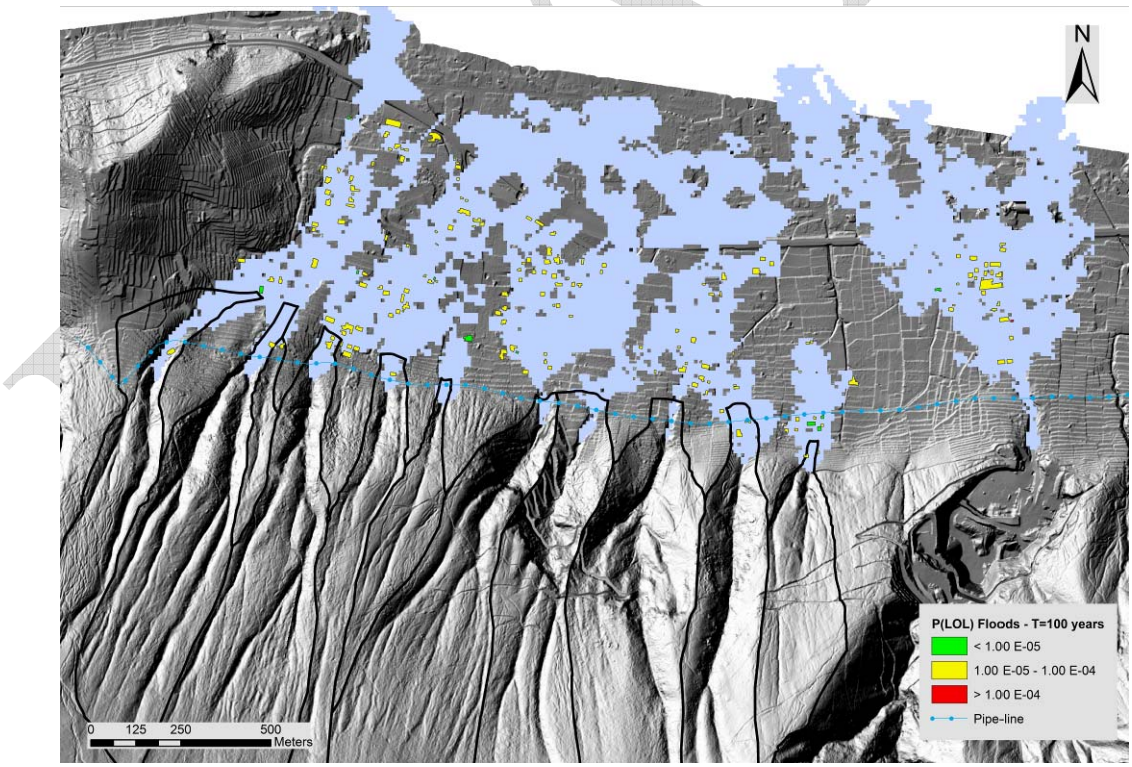

Figure 13. Map of the risk to life loss posed by the flooding phenomena *(modified from the presentation given by Prof. Leonardo Cascini during the 3rd meeting of the participatory process in Nocera Inferiore – June 9, 2011).*

6.5. Societal Risk

The results obtained from QRA analyses can be used also to determine the so-called "societal risk", i.e. *the risk of widespread or large scale detriment from the realization of a defined risk, the implications being that the consequence would be on such a scale as to provoke socio/political response* (Leroi et al., 2005). The estimation of the societal risk allows the achievement of different purposes, among which the ranking of the portions of a given urbanised territory at landslide risk and, thus, the prioritization of the areas needing mitigation measures.

In order to pursue this aim for the problem at hand, the urbanised area at the toe of the Monte Albino massif was previously subdivided in n. 6 sectors whose shape and size were established on the basis of the run-out distance results accomplished via the analyses explained in the previous paragraphs. Then, on the basis of the QRA results obtained – for all the considered flow-like mass movement risk (excluding floods) scenarios – in terms of annual probability of loss of live for the persons living within the exposed houses, the maximum number of equivalent victims (Wong et al., 1997) to be expected for each of the considered sectors was finally assessed. This allowed the ranking of the sectors at risk, as shown in Figure 14.

It is worth noting that the most exposed sectors are those labelled with symbols S2, S5 and S4 where an equivalent number of victims equal to 149, 106 and 78 can be respectively expected.

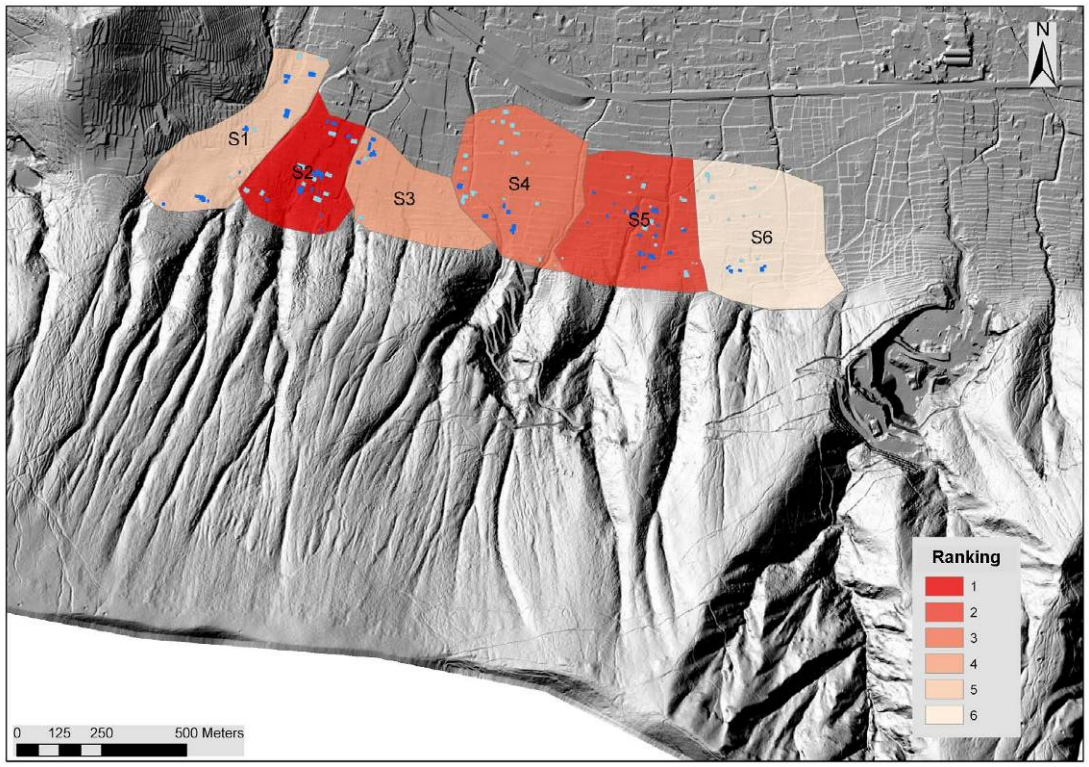

Figure 14. Ranking of the sectors at flow-like mass movement risk established for the urbanised area at the toe of the Monte Albino massif. The houses highlighted in blue are those for which the risk to life loss for the person most at risk living inside is the highest.

References

Baum, R.L., Savage, W.Z., Godt, J.W. 2002. TRIGRS - a FORTRAN program for transient rainfall infiltration and grid-based regional slope-stability analysis. U. S. Geological Survey Open-File Report 02-0424.

Beguinot, C. 1957. La pianificazione urbanistica della Valle del Sarno: questioni di metodo per la valutazione dell'ambiente, Napoli 1957 (in Italian).

Cascini L., Cuomo S., Guida D. (2008) - Typical source areas of May 1998 flow-like mass movements in the Campania region, Southern Italy. Engineering Geology, 96 (3), p.107-125.

Cimmelli, V. 1990. Università, borghesia e popolo a Nocera dei Pagani nei secoli XVII e XVIII, in "Rassegna storica salernitana", VII, 1990/2, pp. 93-116 (in Italian).

Corominas, J., Mavrouli, O. (coordinators) 2011. Guidelines for landslide susceptibility, hazard and risk assessment and zoning. Deliverable 2.4 of the Work Package 2.1 - Harmonization and development of procedures for quantifying landslide hazard. SafeLand Project - 7th Framework Programme Cooperation Theme 6 Environment (including climate change) Sub-Activity 6.1.3 Natural Hazards.

Corominas, J., Copons, R., Moya, J., Vilaplana, J.M., Altimir, J., Amigó, J. 2005. Quantitative assessment of the residual risk in a rockfall protected area. *Landslides*, 2: 343-357.

Corominas, J., Moya, J. (2008). A review of assessing landslide frequency for hazard zoning purposes. Engineering Geology, 102:193-213.

Costa, J.E. 1988. Rheologic, geomorphic, and sedimentologic differentiation of water floods, hyperconcentrated flows, and debris flows. In: V.R. Baker, R.C. Kochel, and P.C. Patton (eds.), Flood Geomorphology, John Wiley and Sons, New York, pp. 113-122.

Dai, F.C., Lee, C.F., Ngai, Y.Y. 2002. Landslide risk assessment and management: an overview. Engineering Geology 64:65-87.

D'Elia, C. 1994. Bonifiche e Stato nel Mezzogiorno (1815-1860), Napoli (in Italian).

Dietrich, W.E., Reneau, S.L., Wilson, C.J., 1986. Hollows, colluvium and landslides in soil-mantled landscapes. In: Abrahamas, A.D. (Ed.), Hillslope processes. Allen and Unwin, pp. 361–388.

De Natale, G., Troise, C., Pingue, F., Mastrolorenzo, G., Pappalardo, L. 2006. The Somma–Vesuvius volcano (Southern Italy): Structure, dynamics and hazard evaluation. Earth-Science Reviews, 74: 73– 111. doi:10.1016/j.earscirev.2005.08.001

Fell, R., Corominas, J., Bonnard, Ch., Cascini, L., Leroi, E., Savage, W.Z. on behalf of the JTC-1 Joint Technical Committee on Landslides and Engineered Slopes 2008. Guidelines for landslide

susceptibility, hazard and risk zoning for land use planning. Engineering Geology, 102: 85-98.

Fell, R., Ho, K.K.S., Lacasse, S., Leroi, E. 2005. A framework for landslide risk assessment and management. In: Hungr O., Fell R., Couture R., Eberhardt E. (eds.) Landslide Risk Management. Taylor and Francis, London, pp. 3-26.

Geotechnical Engineering Office (1998). Landslides and Boulder Falls from Natural Terrain: Interim Risk Guidelines. GEO Report No. 75. Geotechnical Engineering Office, The Government of the Hong Kong Special Administrative Region.

Hungr, O. (1995). A model for the runout analysis of rapid flow slides, debris flows and avalanches. Canadian Geotechnical Journal, 32: 610-623.

Hungr, O., Evans, S.G., Bovis, M.J. & Hutchinson J.N. 2001. A review of the classification of landslides of the flow type. Environmental & Engineering Geoscience, VII (3): 221-238.

Hutchinson, J.N. 1988. Morphological and Geotechnical parameters of Landslides in relation to Geology and Hydrogeology. State of the art Report. Proceedings of the V Int. Symposium on Landslides, Lausanne, Vol. 1, pp. 3 – 35.

Hutchinson, J.N. 2004. Review of flow-like mass movements in granular and fine-grained materials. Proceedings of the Int. Workshop "Flows 2003 - Occurrence and Mechanisms of Flows in Natural Slopes and Earthfill", pp. 3 – 16.

Marciani, F. 1930. Per la bonifica integrale dell'Agro Nocerino. Relazione presentata a S.E. il Prefetto di Salerno. 16.3.1930, Salerno 1930 (in "Il Picentino", giugno 1931) [BNN Misc B 42(24] (in Italian).

Migale, L.S., Milone, A. 1998. Colate di fango in terreni piroclastici della Campania. Primi dati della ricerca storica, Rassegna storica salernitana, n.s., XV/2, , n. 30, dicembre, 235-271 (in Italian).

O'Brien, J.S., Julien, P.Y., Fullerton, W.T. 1993. Two-dimensional water flood and mudflow simulation. Journal of Hydraulic Engineering ASCE, 119(2): 244-261.

Operative Unit 2.38. 1998,. Ricerca storica sulle colate di fango in terreni piroclastici della Campania. G.N.D.C.I.-C.N.R. Report. University of Salerno, Italy (in Italian).

Orlando, G. 1884. Storia di Nocera de' Pagani, voll. 3, Editore Tocco, Napoli (in Italian).

Pucci, R. 1995. Il Vescovado: il casale, gli abitanti, la chiesa. in Radici nocerine. La storia al servizio del futuro, vol. I, Nocera 1995, pp. 49-67 (in Italian).

Rolandi, G., Paone, A., Di Lascio, M., Stefani, G. 2007. The 79 AD eruption of Somma: The relationship between the date of the eruption and the southeast tephra dispersion. Journal of Volcanology and Geothermal Research 169: 87–98. doi:10.1016/j.jvolgeores.2007.08.020

Rossi, F., Villani, P. 1995. Valutazione delle piene in Campania. Pubbl. n. 1470 del GNDCI-CNR.

Scandone, R., Giacomelli, L., Fattori Speranza, F. 2008. Persistent activity and violent strombolian eruptions at Vesuvius between 1631 and 1944. Journal of Volcanology and Geothermal Research, 170: 167–180. doi:10.1016/j.jvolgeores.2007.09.014

Wong, H.N., Ho, K.K.S., Chan, Y.C. 1997. Assessment of consequence of landslides. Proceedings of the International Workshop on Landslide Risk Assessment, Honolulu, Hawaii, USA, pp. 111-149.

Wong, H.N. 2005. Landslide risk assessment for individual facilities. In: Hungr O., Fell R., Couture R., Eberhardt E. (eds.) Landslide Risk Management. Taylor and Francis, London, pp. 237-296.